Mikheev et al., J Nanomater Mol Nanotechnol 2013, 2:4
http://dx.doi.org/10.4172/2324-8777.1000118

Journal of Nanomaterials & Molecular Nanotechnology

Research Article

A SCITECHNOL JOURNAL

Laser Bleaching of Carbon Nanotubes Suspension in *N*,*N*-Dimethylformamide

Konstantin G Mikheev[1]*, Gennady M Mikheev[1], Vladimir L Kuznetsov[2], Tatyana N Mogileva[1], Sergey I Moseenkov[2] and Mariya A Shuvaeva[2]

Abstract

It is shown experimentally that the multiwall carbon nanotubes (MWNTs) suspension in *N*,*N*-dimethylformamide (DMF) irreversibly bleaches in a wide spectrum range under a pulsed nanosecond laser radiation at the wavelength of 532 nm. According to the data of the transmission electron microscopy (TEM), the Raman spectroscopy and the reflection infrared spectrometry the bleaching is shown to be caused by MWNTs degradation, with the formation of new chemical bonds which result from the laser-induced chemical reactions between MWNTs and DMF molecules.

Keywords

Carbon nanotubes; Suspension; Photochemical reactions; Photo-induced bleaching

Introduction

Scientists have recently been studying light and nanocarbon materials interaction to acquire new knowledge to develop radically new devices for photonics and optoelectronics, e.g. graphene mode-locked laser [1] and passive laser switches based on suspensions and films of single-wall carbon nanotubes (SWNTs), permitting to obtain laser picosecond and subpicosecond pulses in the infrared region [2-8]. One can also cite the study of the laser radiation interaction with nanographite films that resulted in creation of a quick-response photodetector which can operate in a wide spectral range [9] at high temeperatures [10]. A fundamentally new type of a polarization analyzer of laser radiation on the basis of this study has been designed and made [11], the principle of operation being the recording of the polarization-dependent surface photocurrents in nanographite films.

The study of laser radiation interaction with nanocarbon materials is also of interest from the point of view of production of new organic materials possessing different magnetic properties [12,13], magnetooptical light modulators developing [13], improvement of optical limiters based on nanocarbon materials [14-17]. Research in this field is also useful as an approach to locally engineer the band gap and defect densities along the SWNTs [18].

We have recently shown the semitransparent onion-like carbon (OLC) suspension in *N*,*N*-dimethylformamide (DMF) to irreversibly bleach under high light fluence at the wavelength of 1064 nm, with the bleached fraction possessing pronounced diamagnetic properties [19]. We explained it by the laser-induced chemical reactions between OLC and DMF (graphene shells hydrogenation with formation of non-conducting fragments resembling condensed aromatic compounds) resulting in the transparent liquid formation. The photo-induced reactions between fullerenes and H-donor molecules in presence of photosensitizers were previously observed [20]. Besides, the reaction of SWNTs with hydrogen gas in the temperature range of 400-550°C and under the hydrogen pressure of 50 bar was reported [21]. The photo-induced chemical reactions of SWNTs with oxygen were also observed [22]. In that study it is shown that laser radiation causes pronounced bleaching and decay of photoluminescence from SWNTs on either glass or mica substrates. To put it another way and to take into account the fact that MWNTs can absorb the electromagnetic radiation in the wide wave band [23], it is logical to expect similar phenomena such as in the suspension of OLC in DMF to occur in the suspension of MWNTs in DMF under the laser radiation effect. In this paper we report on the study of the laser radiation interaction with this suspension.

Experimental Section

The MWNTs obtained by CVD technology in the reaction of the ethylene thermal catalytic decomposition on the Fe/Co catalysts were used in experiments. The MWNTs average diameter and length were 7-9 nm and 10-20 μm respectively (Figure 1a and 1b). The suspension of tubes in DMF with the MWNTs concentration of 0.015 g/l was dispersed ultrasonically (22 kHz, 300 W). This suspension was stable for 24 hours.

The optical scheme of this experiment is presented in Figure 2a. Laser beam of the YAG:Nd^{3+}-laser with a frequency converter into second harmonic (the wavelength of 532 nm, the pulse duration of 17 ns) [24] passed through opened shutter (1) was focused by lens (2), with a focal distance of 100 mm, on an optical cuvette filled with the suspension under study (3). At closed shutter (1), the region of interaction between laser radiation and suspension (3) was photographed by photocamera (4). The diameter of the focused beam waist was 70 μm and the thickness of the cuvette was 1 mm.

To measure the transmission spectrum of the initial and bleached suspensions, the suspensions samples were placed in a 1.01-mm quartz cuvette. The measurements were made by the PerkinElmer LAMBDA 650 double-beam UV/Vis spectrophotometer.

The transmission electron microscope JEM 2012 (JEOL, Japan) with the accelerating voltage of 200 kV was used to obtain high resolution TEM images of the MWNTs and particles of the bleached suspension. The lattice plane resolution was 0.14 nm and the point resolution was 0.194 nm.

The comparative analysis of the products contained in the initial and bleached suspensions has been carried out by the Raman spectrometer (Labram HR800, Horiba) at the wavelength of 632.8 nm and by the infrared reflectance spectrometer (FTIR 8000, Shimadzu). Thereto the films containing the solid fractions of the suspensions

***Corresponding author:** Konstantin G Mikheev, Institute of Mechanics of Ural Branch of Russian Academy of Sciences, 34 ul. T. Baramzinoy, 426067 Izhevsk, Russia, E-mail: k.mikheev@udman.ru

Received: July 01, 2013 **Accepted:** August 13, 2013 **Published:** August 20, 2013

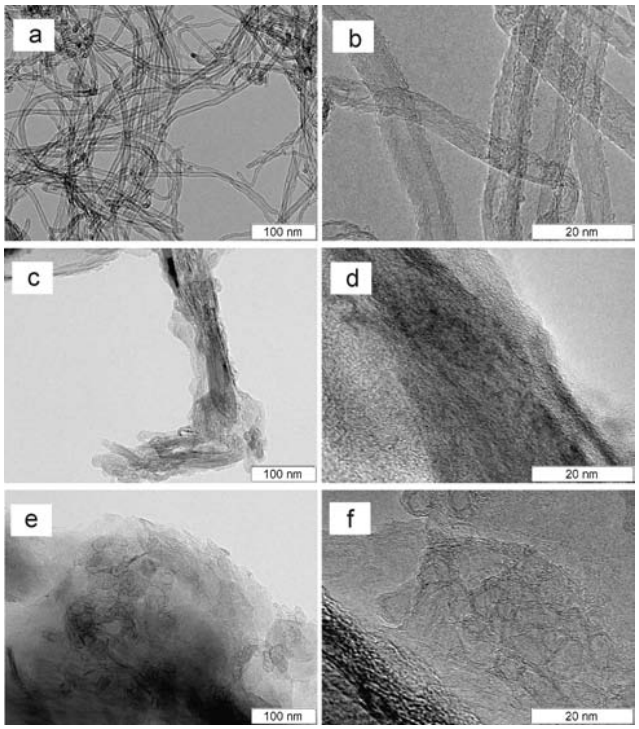

Figure 1: TEM images of the (a, b) initial MWNTs samples and (c, d, e, f) particles of the bleached suspension. (c) The tubes remains with amorphized external layers, (d) a big graphite-like fragment, (e) the fragments of nanotubes and capsules of multi-wall graphene-like layers, (f) the remains of tubes walls (2-3 layers).

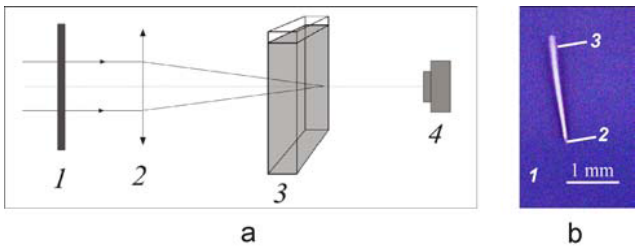

Figure 2: (a) The optical scheme of the experiment: (1) - shutter; (2) - focusing lens; (3) - optical cuvette with MWNT suspension in DMF; (4) - photocamera; (b) the image of the bleached part of the suspension: (1) suspension, (2) zone under irradiation (a focused laser beam was perpendicular to the image plane), (3) bleached suspension spreading upwards by virtue of thermal convection.

were produced on a quartz substrate by a simple exsiccation of a suspension layer deposited on the substrate.

Results and Discussion

The MWNT suspension was treated by pulsed laser radiation at different values of the input fluence *W*. The maximum value of the input fluence was below 2 J·cm^{-2}. The bleaching was observed after the action of several pulses. The input fluence *W* of these pulses was above 0.8 J·cm^{-2}. A typical image of the suspension bleached part is shown in Figure 2b. From this figure one can see that the bleached fraction of the suspension formed by the absorbed laser power, and therefore having a higher temperature, moves upward in the vertical direction.

To understand and analyze the bleaching mechanisms of the suspension, it was necessary to obtain the bleached fraction of the suspension in *quantum satis*. To this end the initial MWNTs suspension in DMF after its dispersion was injected into the optical cuvette and exposed to laser pulses for a long time, with the pulse repetition rate of 1 Hz, during 75×10^3 s. As a result initial semitransparent suspension was transformed into a practically transparent liquid.

The bleached fraction of the suspension had a yellowish shade. The optical density of initial χ_1 (blue line) and bleached χ_2 (green line) suspensions as functions of the light wavelength (λ) obtained relative to DMF are shown in Figure 3. From these measurements one can see that the bleaching phenomenon occurs over the whole range of the wave band from 200 to 900 nm, since the inequality $\chi_1(\lambda)>\chi_2(\lambda)$ is true. However, from the calculated dependence ($\chi_2/\chi_1(\lambda)$) which is shown in the inset in Figure 3 one can conclude that the degree of bleaching depends on the wavelength. Laser bleaching reveals itself strongly over the wave bands of 330<λ<900 nm and 200<λ<250 nm. The total bleaching was established to occur at the wavelength range of 615<λ<900 nm. The bleaching at the wavelength range of 250<λ<330 nm is less pronounced since the χ_2/χ_1 ratio exceeds 0.5 over this wave band. It defines a weak yellowish shade of the bleached suspension obtained.

It was of interest to perform a comparative spectral analysis of materials contained in the initial and bleached suspensions using the Raman spectroscopy and the infrared reflectance spectrometry. The Raman spectrum of the initial MWNTs particles (prior to dispersion) was also obtained.

The study has shown that the Raman spectrum of the initial particles of MWNTs and samples of the MWNTs suspension practically does not differ in the frequency shifts region 1000-1800 cm^{-1}. The scattering spectrum of the initial MWNTs consists of two peaks with the frequency shifts of 1594.1 cm^{-1} (G band) and 1335.4 cm^{-1} (D band) (Figure 4a). The presence of the D band, with the intensity being greater than that of the G band, is associated with the presence of impurities and a lot of defects in the MWNTs studied [25].

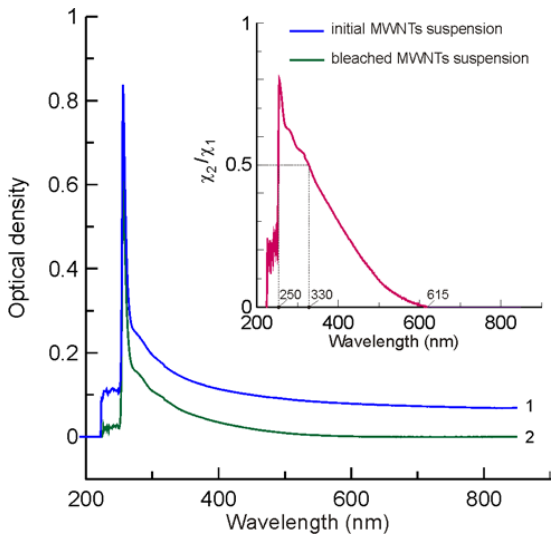

Figure 3: The optical density of χ_1 (1) initial and χ_2 (2) bleached suspensions as functions of the λ light wavelength obtained relative to DMF. The suspensions were kept in quartz cuvettes with thickness of 1.01 mm. The $\chi_2/\chi_1(\lambda)$ calculated dependence is shown in the inset.

From Figure 4b one can see that the Raman spectrum of the film obtained from the bleached fraction of the studied suspension differs considerably from that of the initial MWNTs (Figure 4a) suspension and DMF (Figure 4c). According to the reference data [26], the scattering peaks of the bleached fraction with the frequency shifts of 1074 and 1460.2 cm^{-1} are due to the CH_2 bonds, and the peak with the shift of 1138 cm^{-1} corresponds to the CH_3 bonds. The esters (-COOR) or aldehydes (-CHO) or carboxylic acids (-COOH) can cause a peak with the shift of 1739.9 cm^{-1}. The peak with the shift of 1613.5 cm^{-1} can be conditioned by the $-NH_2$ group. The investigations carried out by the infrared spectrometer also confirm the presence of the chemical bonds in the bleached fraction of the suspension (Figure 5). Thus, the peaks with the shifts of 2963 cm^{-1}, 2933 cm^{-1}, 2876 cm^{-1}, 1468 cm^{-1} correspond to the CH_3 bonds, the peaks with the shift of 1748 cm^{-1} – to the lactones, the peaks with the shifts of 1163 cm^{-1} and 1059 cm^{-1} – to the ethers (R-O-C-O-R). It is difficult to interpret the peaks with the shifts of 816 cm^{-1}, 713 cm^{-1}, 650 cm^{-1}, 541 cm^{-1}. However, one can attribute the frequency range 720-740 cm^{-1} to the methylene groups ($-CH_2-CH_2-$). The peaks with the shifts of 3400-3500 cm^{-1} and 1600 cm^{-1} were not observed in the infrared spectrum of bleached MWNTs suspension. These frequency ranges are typical for NH groups, so we can conclude that the dimethylformamide group is not present in the bleached MWNTs suspension. We should note that it was difficult to set off the effect of the background, so the peaks with the shifts of 2363 cm^{-1} and 2343 cm^{-1} correspond to CO_2.

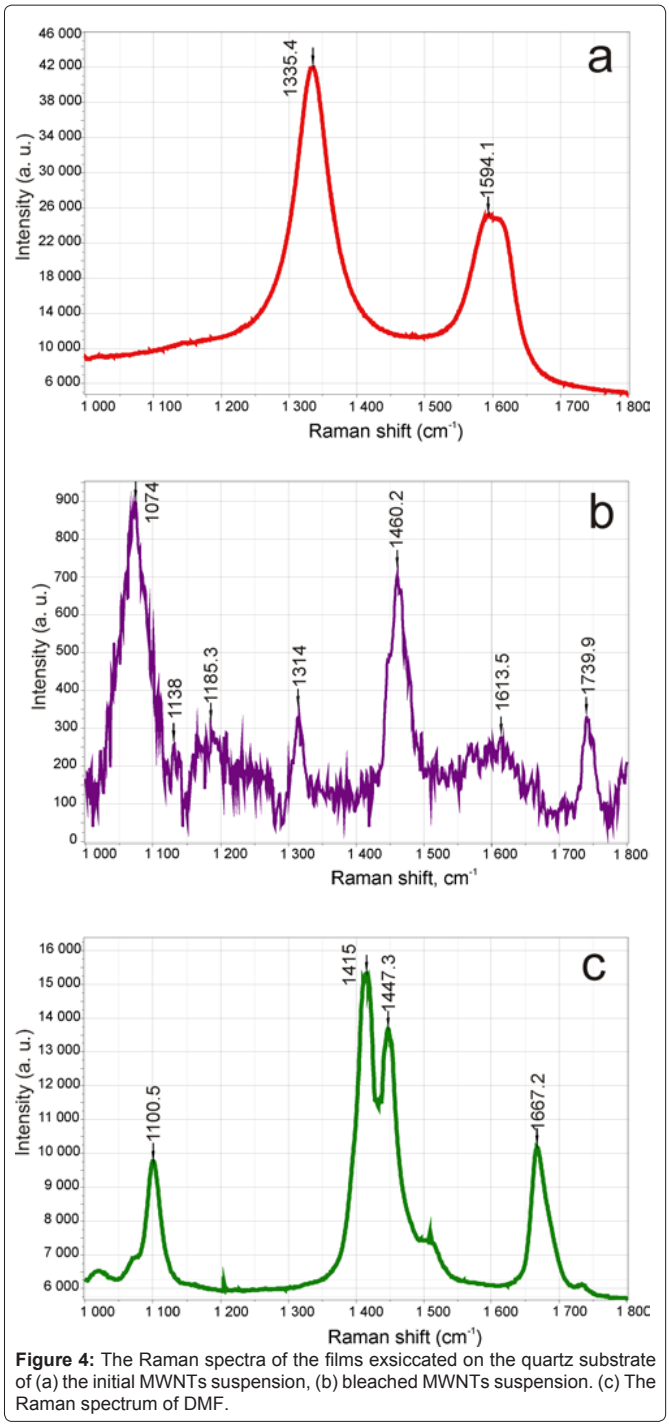

Figure 4: The Raman spectra of the films exsiccated on the quartz substrate of (a) the initial MWNTs suspension, (b) bleached MWNTs suspension. (c) The Raman spectrum of DMF.

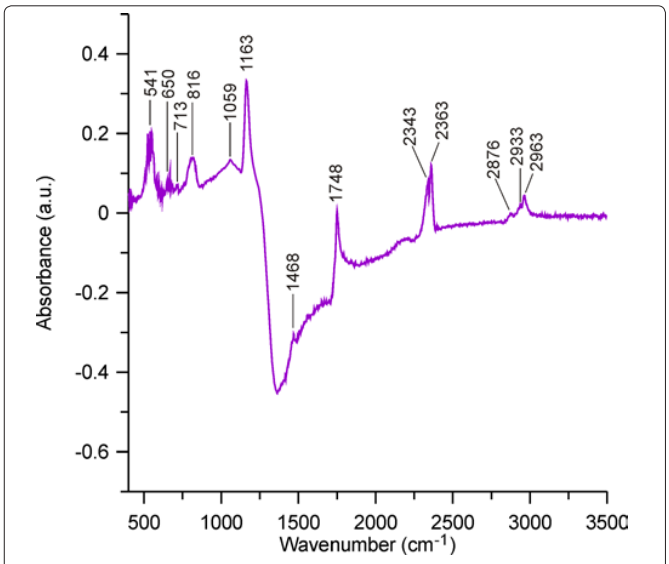

Figure 5: The infrared spectrum of bleached MWNTs suspension.

The TEM study of the bleached fraction of suspension has shown the bleached fraction to consist of an inhomogeneous mixture of different carbon formations (Figure 1c-1f). It can be divided into graphite-like aggregates, polyhedral thin-walled formations and amorphized carbon-bearing remains of an organic solvent. A great amount of carbon is concentrated in large (several microns) graphite-like particles consisting of bundles of graphene layers, with the thickness of 5-20 nm. In addition, the polyhedral fragmented remains of carbon nanotubes with the length of 5-20 nm are observed. The graphene walls quantity of such fragments is 2-10. The formations remotely resembling the fragments of MWNTs are also present. The organic remains of the solvent localize on the graphite layers surface and cover the polyhedral formations. The film thickness ranges from 0.5 nm to 3 nm. These data indicate that the photochemical reactions between MWNTs and DMF in the suspension of MWNTs in DMF occur under the laser exposure, which results in the formation of new chemical bonds which are not present in the initial suspension.

Conclusions

We have reported the phenomenon of the bleaching of MWNTs suspension in DMF under the powerful laser radiation effect at the wavelength of 532 nm, which reveals itself after several laser

pulses. The suspension bleaches in the wide wave band from 200 to 900 nm. The bleaching results from the photochemical reactions between MWNTs and DMF, which leads to the formation of a new stable liquid fraction. It was verified by the analysis of the initial and bleached fractions of the suspension using the transmission electron microscopy, the infrared spectrometry and the Raman spectroscopy. Although presented results demonstrate that the powerful laser irradiation destroys the graphitic structure of the MWNTs we believe that there is a proper value of laser intensity for functionalizing the MWNTs by different groups of H-donor compounds.

Acknowledgements

This work was supported by UB RAS grant no. 12-C-1-1003, RFBR grant no. 12-02-31724 and by The Ministry of education and science of Russian Federation, project no. 8748 from 01.10.2012.

References

1. Bao Q, Zhang H, Ni Z, Wang Y, Polavarapu L, et al. (2011) Monolayer Graphene as a Saturable Absorber in a Mode-Locked Laser. Nano Res 4: 297-307.
2. Yamashita S, Inoue Y, Maruyama S, Murakami Y, Yaguchi H, et al. (2004) Saturable absorbers incorporating carbon nanotubes directly synthesized onto substrates and fibers and their application to mode-locked fiber lasers. Opt Lett 29: 1581-1583.
3. Song YW, Set SY, Yamashita S, Goh CS, Kotake T (2005) 1300-nm pulsed fiber lasers mode-locked by purified carbon nanotubes. IEEE Photonics Technol Lett 17: 1623-1625.
4. Il'ichev NN, Obraztsova ED, Pashinin PP, Konov VI, Garnov SV (2004) Self-mode locking in a F_2^-:LiF laser by means of a passive switch based on single-wall carbon nanotubes. Quantum Electron 34: 785.
5. Wang F, Rozhin AG, Scardaci V, Sun Z, Hennrich F, et al. (2008) Wideband-tuneable, nanotube mode-locked, fibre laser. Nat Nanotechnol 3: 738-742.
6. Kivistö S, Hakulinen T, Kaskela A, Aitchison B, Brown DP, et al. (2009) Carbon nanotube films for ultrafast broadband technology. Opt Express 17: 2358-2363.
7. Qin HB, Wang YG, Zhang HB, Liu J, Zhuo Z (2012) A passively mode-locked Nd:YVO_4 laser with a carbon nanotube saturable absorber. Laser Phys 22: 684-687.
8. Iliev H, Buchvarov I, Choi SY, Kim K, Rotermund F, et al. (2012) Steady state mode-locking of a 1.34 μm Nd:YVO4 laser using a single-walled carbon nanotube saturable absorber. Appl Phys B: Lasers Opt 106: 1-4.
9. Mikheev GM, Zonov RG, Obraztsov AN, Volkov AP, Svirko YP (2006) Quick-response film photodetector of high-power laser radiation based on the optical rectification effect. Tech Phys 51: 1190-1196.
10. Mikheev GM, Zonov RG, Obraztsov AN, Svirko YP (2009) Efficiency of a fast-response nanographite-based optoelectric converter in air at high temperatures. Tech Phys Lett 35: 899-902.
11. Mikheev GM, Styapshin VM (2012) Nanographite analyzer of laser polarization. Instrum Exp Tech 55: 85-89.
12. Makarova TL, Han KH, Esquinazi P, Da Silva RR, Kopelevich Y, et al. (2003) Magnetism in photopolymerized fullerenes. Carbon 41: 1575-1584.
13. Mikheev KG, Mogileva TN, Mikheev GM, Kuznetsov VL, Moseenkov SI (2012) Diamagnetism appearance of onion-like carbon suspension by laser radiation. Mater. Phys. Mech. 13: 37-47.
14. Jin Z, Huang L, Goh SH, Goh G, Goh W (2002) Size-dependent optical limiting behavior of multi-walled carbon nanotubes. Chem Phys Lett 352: 328-333.
15. Liu ZB, Tian JG, Guo Z, Guo DM, Du F, et al. (2008) Enhanced optical limiting effects in porphyrin-covalently functionalized single-walled carbon nanotubes. Adv Mater 20: 511-515.
16. Wang J, Blau WJ (2008) Nonlinear optical and optical limiting properties of individual single-walled carbon nanotubes. Appl Phys B: Lasers Opt 91: 521-524.
17. Lim GK, Chen ZL, Clark J, Goh RGS, Ng WH, et al. (2011) Giant broadband nonlinear optical absorption response in dispersed graphene single sheets. Nat Photonics 5: 554-560.
18. Finnie P, Lefebvre J (2012) Photoinduced band gap shift and deep levels in luminescent carbon nanotubes. ACS Nano 6: 1702-1714.
19. Mikheev GM, Mikheev VL, Mikheev KG, Mogileva TN, Moseenkov SI (2011) Laser-induced diamagnetism in suspension of onion-like carbon particles. Tech Phys Lett 37: 831-834.
20. Siedschlag C, Luftmann H, Luftmann C, Luftmann J (1999) [60]Fullerene Radical Cation: Reactions and Mechanism. Tetrahedron 55: 7805-7818.
21. Talyzin AV, Luzan S, Anoshkin IV, Nasibulin AG, Jiang H, et al. (2011) Hydrogenation, purification, and unzipping of carbon nanotubes by reaction with molecular hydrogen: road to graphane nanoribbons. ACS Nano 5: 5132-5140.
22. Georgi C, Hartmann N, Gokus T, Green AA, Hersam MC, et al. (2008) Photoinduced luminescence blinking and bleaching in individual single-walled carbon nanotubes. Chemphyschem 9: 1460-1464.
23. Kuznetsov VL, Moseenkov SI, Elumeeva KV, Larina TV, Anufrienko VF, et al. (2011) Comparative study of reflectance properties of nanodiamonds, onion-like carbon and multiwalled carbon nanotubes. Phys. Status Solidi B 248: 2572-2576.
24. Mikheev GM, Mogileva TN, Popov YA, Kaluzhny DG (2003) A computer-based laser system for the diagnostics of hydrogen in gas mixtures. Instrum Exp Tech 46: 233-239.
25. Bokova SN, Obraztsova ED, Grebenyukov VV, Grebenyukov KV, Ishchenko AV, et al. (2010) Raman diagnostics of multi-wall carbon nanotubes with a small wall number. Phys Status Solidi B 247: 2827-2830.
26. Dean JA (1999) Lange's handbook of chemistry. McGraw-Hill, Inc., New York, USA.

Author Affiliations

Top

[1]*Institute of Mechanics of Ural Branch of Russian Academy of Sciences, 34 ul. T. Baramzinoy, 426067 Izhevsk, Russia*
[2]*Boreskov Institute of Catalysis Siberian Branch of Russian Academy of Sciences, 5 Akad. Lavrent'ev prosp., 630090 Novosibirsk, Russia*